Ethanol catalytic deposition of MoS_2 on tapered fiber

Hao Wang,[1] Bohua Chen,[1] Xiaoyan Zhang,[2] Sheng Liu,[1] Bangqi Zhu,[1] Jun Wang,[2] Kan Wu,[1,*] and Jianping Chen[1]

[1]*State Key Laboratory of Advanced Optical Communication Systems and Networks, Department of Electronic Engineering, Shanghai Jiao Tong University, Shanghai 200240, China*
[2]*Key Laboratory of Materials for High-Power Laser, Shanghai Institute of Optics and Fine Mechanics, Chinese Academy of Sciences, Shanghai 201800, China*
**Corresponding author: kanwu@sjtu.edu.cn*

Received January 6, 2015; revised February 15, 2015; accepted March 4, 2015; posted March 6, 2015 (Doc. ID 231621); published June 1, 2015

Deposition of two-dimensional (2D) MoS_2 materials on the tapered fiber allows various photonic applications including saturable absorbers and four-wave mixing. Ethanol catalytic deposition (ECD) of MoS_2 on the optical tapered fiber was proposed and demonstrated in this work. Different from the conventional optical driven deposition using water or organic solvent, the ECD method utilized the high volatility of the ethanol solvent, which significantly increased the movement speed of the MoS_2 nanosheets and thus boosted the deposition rate and reduced the minimum power threshold to drive the deposition. We believe the ECD method should be able to be applied to other similar 2D materials such as other types of transition metal chalcogenides.

OCIS codes: (160.4330) Nonlinear optical materials; (310.1860) Deposition and fabrication; (230.4320) Nonlinear optical devices.
http://dx.doi.org/10.1364/PRJ.3.00A102

1. INTRODUCTION

With the discovery of graphene, two-dimensional (2D) materials have received intense interest for their abundant electronic and photonic properties [1–4]. These materials include graphene, graphene oxide, topological insulators, and transition metal dichalcogenides (TMDs). The tunable bandgap and absorption of the 2D materials have been utilized for optical intensity modulation [5]. The wideband absorption spectrum has been reported to allow the operation of a broadband polarizer [6]. Among various applications, the nonlinear properties of the materials have been paid special attention. One nonlinear property is the saturable absorption, which means the transmission of the material is dependent on the incident optical intensity [3]. The beam with higher intensity would experience higher transmission; i.e., the absorption is saturated. This effect is due to the Pauli block, which means that the conduction band of the materials can be fully filled by the optoelectrons and no more light would be absorbed after the saturation. Saturable absorption is key for the applications of mode-locked lasers and *Q*-switched lasers. The demonstrations of mode-locking and *Q*-switching operations based on many different 2D materials have been extensively investigated due to their advantages of wide operation wavelength, compact size, easy fabrication, and controllable saturation parameters [7–17]. Another important nonlinear property is the optical nonlinearity, namely $\chi^{(3)}$ or n_2 [18,19]. Optical nonlinearity allows the realization of four-wave mixing, which has wide applications including wavelength conversion, frequency comb generation, and microwave photonic filtering [20]. It has been reported that graphene has optical nonlinearity much higher than that in a conventional silica fiber, which indicates its potential to be a highly compact nonlinear device [19]. Recently, molybdenum disulfide (MoS_2) together with other types of TMDs has been reported to exhibit comparable optical nonlinearity with graphene, which further extended the choice of nonlinear optical materials [9,18,21].

On the other hand, incorporation of the 2D materials into the well-developed fiber systems is important because it would explore the promising properties of the 2D materials together with the mature technologies of the fiber systems. Different incorporation methods have been developed, including directly transferring the CVD grown 2D materials to the fiber end [1,2], depositing to the fiber end [22,23], depositing to the fiber waist of the tapered fiber or side polished fiber [12,15], and embedding into the polymer thin film [16,24]. Among all these methods, deposition of the 2D materials to the fiber waist of the tapered fiber has its own merit; that is, the interaction length between the light beam and the materials can be very long, from a few hundreds of micrometers to a few centimeters. This property enables the control of the saturation parameters if used as a saturable absorber, and the enhancement of four-wave mixing if used as a nonlinear optical device. In the deposition process, a usual method is to apply an optical field between the fiber and the material dispersions so that the small material particles can be attracted by the optical force and attached to the fiber waist or fiber end [25]. Although there have been a few works discussing the deposition technology, we found that in all these works the solvents of the material dispersions were only used to disperse the materials and had little contribution to the deposition process. Moreover, the power threshold for the deposition was usually high, e.g., >10 dBm, because the optical force has to be powerful enough to overcome the resistance from the viscousness of the solvent such as N,N-Dimethyl formamide (DMF) so that the material particles in the solvent

can be given enough acceleration and movement speed to be successfully attached to the fiber waist or fiber end.

In this paper, we proposed and demonstrated a new concept of deposition; i.e., the solvent participates in the deposition process, called ethanol catalytic deposition (ECD), because ethanol was found to be an optimal choice of solvent in the demonstration. The demonstration of deposition of MoS_2–ethanol dispersions to the tapered fiber exhibited a much faster deposition rate than the conventional solvents such as water with surfactant and organic solvent. Moreover, the ECD method allowed a much lower threshold of minimum injected optical power of only 4 dBm to drive the deposition. The key difference was in the high volatility of the ethanol, which significantly enhanced the Brownian motion of the material particles in the dispersions. The randomly oriented Brownian motion became highly oriented toward the tapered fiber with the existence of optical field, which led to a much faster deposition rate and a lower deposition power threshold. Not limited to MoS_2, we believe that the ECD method should also benefit the deposition of other 2D materials such as other types of TMDs.

2. PREPARATION OF MoS_2 DISPERSIONS

Optical driven deposition of MoS_2 on tapered fiber requires the preparation of MoS_2 dispersions. The liquid-phase exfoliation (LPE) method was utilized, which can produce monolayer and few-layer MoS_2 nanosheets with large quantity. Moreover, LPE requires no chemical processing on the material and thus can produce chemically pristine MoS_2 nanosheets. In the experiment, ~0.02 g MoS_2 powder was mixed with 20 mL 95% ethanol and was sonicated for 1 h to generate MoS_2 nanosheets. Then the MoS_2–ethanol mixture was centrifuged for 90 min to separate the nanosheets with unexfoliated large-size flakes. The top 2/3 dispersions were collected for experimental use. Figure 1(a) shows the procedures of preparation of MoS_2–ethanol dispersions. Figures 1(b) and 1(c) show the transmission electron microscope (TEM) images of MoS_2 nanosheets with two different scales. It can be seen that the typical size of MoS_2 nanosheets was a few hundreds of nanometers, and in a region a few tens of nanometers wide the nanosheets showed good uniformity.

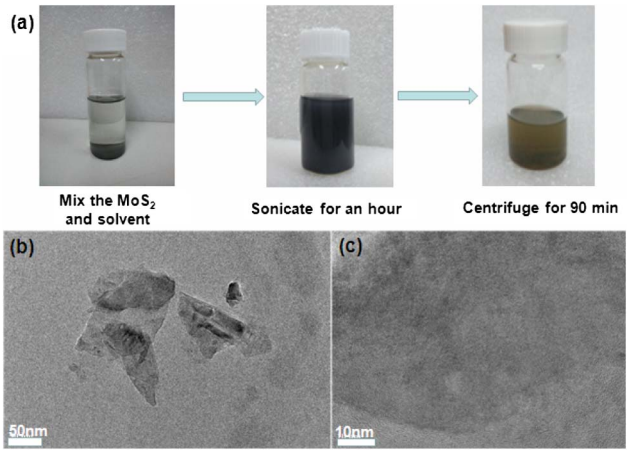

Fig. 1. (a) Procedures of preparation of MoS_2–ethanol dispersions. (b) TEM image of MoS_2 nanosheets with 50 nm scale bar. (c) High-resolution TEM image with 10 nm scale bar.

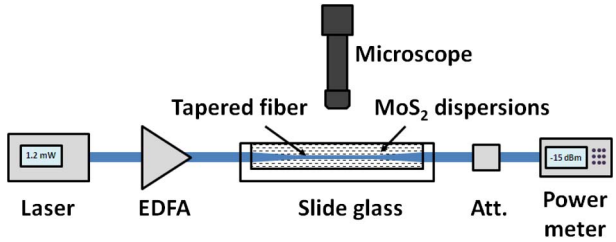

Fig. 2. Experimental setup for ethanol catalytic MoS_2 deposition on tapered fiber.

3. EXPERIMENTAL RESULTS

The experimental setup for MoS_2 deposition on the tapered fiber is shown in Fig. 2. The experiments were all performed under the room temperature of 25°C. The light near 1550 nm was generated from a continuous wave (cw) laser source and amplified by a commercial erbium-doped fiber amplifier (EDFA) to near 15 dBm. The tapered fiber was placed inside a slot of a customized slide glass and immersed in the prepared MoS_2–ethanol dispersions. The light was injected into one side of the tapered fiber, and the output on the other side of the tapered fiber was monitored by an optical power meter after a 20 dB attenuator. The use of attenuator was to meet the measurement range of the power meter. A long-focal-length microscope with a resolution of ~1 μm and a view of field of ~2 cm was vertically placed on the top of the tapered fiber to monitor the deposition process. Although this setup was very similar to a conventional setup for optical driven deposition, the difference lay in the use of ethanol as a solvent. Conventional optical driven deposition mainly utilizes the optical force to attract the material particles, whereas the solvent itself does not contribute to the deposition process. However, in our experiment, ethanol is highly volatile. The volatile process of ethanol can significantly increase the Brownian motion of the MoS_2 nanosheets in the dispersions. With the existence of optical force, i.e., when the optical power was injected into the tapered fiber, the randomly oriented Brownian motion became highly oriented toward the tapered fiber, which resulted in the increase of deposition rate with nearly no effect on the deposition quality.

When the deposition process began, the output power detected by the optical power meter continuously decreased, which meant the loss of the tapered fiber gradually increased due to the deposition. A typical evolution of the optical loss with respect to the deposition time is shown in Fig. 3(a) for a tapered fiber with 10 μm diameter and 15 dBm input optical power. The loss was normalized to 0 dB before the deposition. The MoS_2 deposited tapered fiber did not show polarization-dependent loss, and the thermal damage threshold is ~500 mW tested by a high-power EDFA. The tapered fiber was adiabatic with a typical loss of less than 0.5 dB. A microscope image of the deposition is shown in the inset of Fig. 3(a). It can be observed that the materials have been successfully deposited onto the tapered fiber. To confirm the deposition of MoS_2, the Raman spectral measurement was performed, shown in Fig. 3(b). It should be mentioned that the tapered fiber was moved onto a clean slide glass for the Raman spectral analysis so that the residual MoS_2 in the slot would not affect the measurement results. For comparison, the MoS_2 nanosheets in the dispersions were also

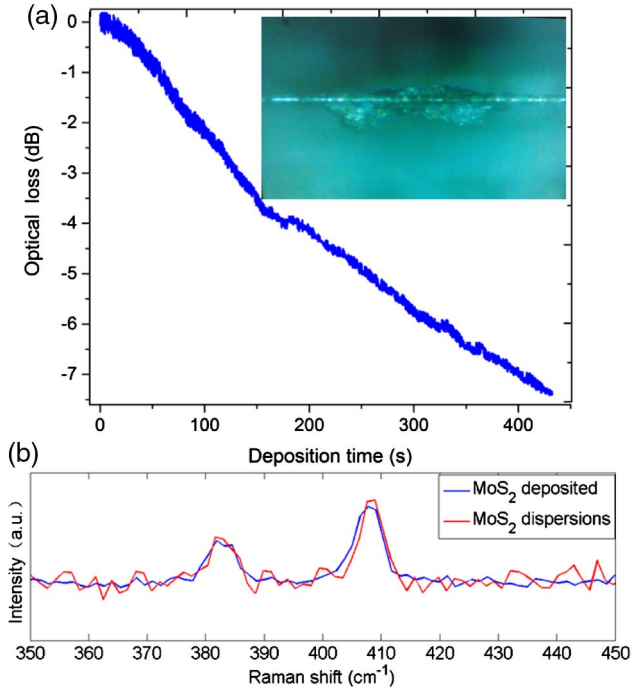

Fig. 3. (a) Typical evolution of the optical loss during the deposition of MoS_2. Inset: microscope image of the deposited MoS_2. (b) Raman spectra of MoS_2 in the dispersions and deposited on the tapered fiber.

measured, shown in Fig. 3(b). It can be seen that the deposited materials have nearly identical Raman spectra compared with the MoS_2 nanosheets in the dispersions, which clearly confirmed the deposition of MoS_2 nanosheets on the tapered fiber.

To compare the effects of different solvents in the deposition process, four solvents with different evaporation rates were used, i.e., water (62 with reference to butyl acetate), DMF (17), ethanol (203), and acetone (1120). The diameters of the tapered fibers were fixed to 10 μm, and the input optical power was fixed to 15 dBm. The measurement results are shown in Fig. 4. It can be observed that the deposition rate of MoS_2–ethanol dispersions was 2.6 times higher than that of MoS_2–DMF and 8.9 times higher than that of MoS_2–water dispersions, which clearly demonstrated the contribution of ethanol as a volatile solution in the deposition process. The higher deposition rate of DMF compared with water is probably due to the fact that DMF has closer surface energy to the MoS_2 and can disperse MoS_2 more uniformly than water. This results in stronger interaction between MoS_2 and DMF molecules in the evaporation process and thus a higher deposition rate. It can also be observed that MoS_2–acetone dispersions had the fastest deposition rate due to the even higher volatility of acetone. However, the high volatility made the Brownian motion of the MoS_2 nanosheets very fast, which can remove the deposited MoS_2 nanosheets when they collide with free-moving MoS_2 nanosheets. This effect resulted in fluctuation of the readings from the power meter. Moreover, it became more difficult to control the deposition to a specific loss level, e.g., 10 dB loss induced by the deposited materials, due to the over-fast deposition rate. The deposition rates of four different solutions are summarized in Table 1. To further clarify, the movement speeds of the MoS_2 nanosheets in the different solvents are also summarized in Table 1. The movement speed

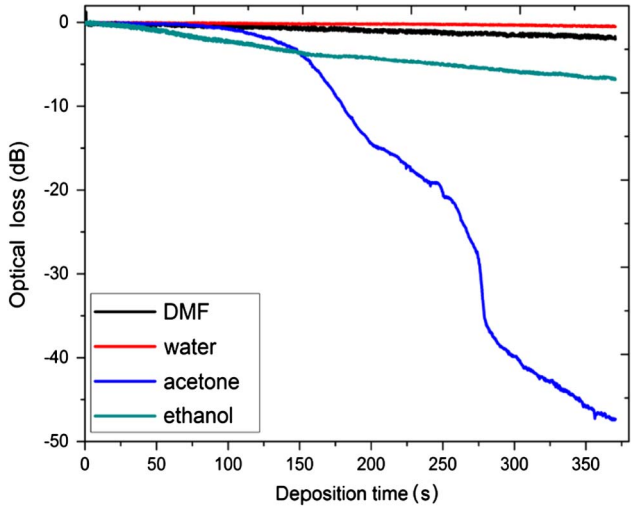

Fig. 4. Deposition process using water, DMF, ethanol, and acetone as solvent.

was estimated by monitoring the movement of some large-size MoS_2 flakes in the dispersions using a microscope. The actual speed of the nanosheets can be even faster, but the trend should be unchanged. It can be clearly seen that a solvent with higher volatility led to a higher movement speed of the MoS_2 nanosheets. Based on the above analysis, it can be concluded that, from the view of deposition, ethanol is an optimal choice of solvent compared with the other three solvents.

In addition, we have studied the different concentration of ethanol aqueous solution and found that the reduction of the ethanol concentration indeed reduced the volatility and resulted in a lower deposition rate. In fact, a mixture of two liquids, such as ethanol and water, can lead to a time-dependent deposition rate, which makes deposition difficult to control, because two liquids have different evaporation rates and the concentration of the mixture changes with time. This is the reason why we used nearly pure liquid in the experiment to guarantee a stable deposition process.

Another important parameter in the deposition is the optical power injected into the tapered fiber. To show the influence of different optical power levels on the deposition process, we decreased the optical power from 15 to 0 dBm with the step of 1–2 dB during a deposition process, shown in Fig. 5(a). The diameter of the tapered fiber was 6 μm. The change of the deposition rate could be clearly observed when the optical power was changed. The dips on the curve at the deposition times of 400, 500, 600, and 700 s were due to the properties of the EDFA when its output power was changed. The inset of Fig. 5(a) shows the evolution of the optical loss when the EDFA was turned off and turned on again, and the supplementary medium shows the movement of MoS_2 nanosheets with the light on (time: 0–2.5 s) and off (time: 2.5–5 s).

Table 1. Deposition Rates and Movement Speeds of the MoS_2 Nanosheets for Different Solvents

Solvent	Water	DMF	Ethanol	Acetone
Deposition rate (dB/s)	0.0018 ±0.0003	0.006 ±0.004	0.016 ±0.004	0.139 ±0.047
Movement speed (μm/s)	~210	~470	~980	~11200

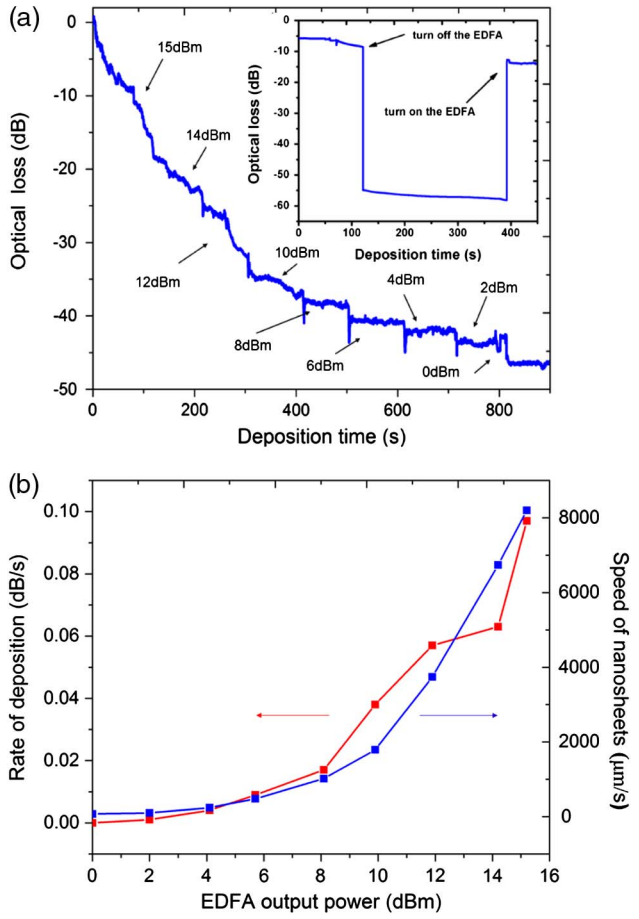

Fig. 5. (a) Deposition process under different injected optical power levels. Inset: evolution of optical loss when the EDFA was turned off and turned on again (see Media 1 in detail). (b) Deposition rate and the movement speed of the MoS_2 nanosheets with respect to the injected optical power.

The difference of the movement speed and movement orientation can be clearly observed. Based on the experimental results, the minimum injected optical power to drive the deposition can be as low as 4 dBm, and the power range to drive the deposition can be as wide as 11 dB. In contrast, the minimum injected power for the conventional optical driven deposition was typically more than 10 dBm, whereas the power range was also narrow, e.g., a few decibels. This means the ECD method allows the deposition to be more easily realized. To understand the origin of this power-dependent deposition rate, we estimated the movement speed of the MoS_2 nanosheets under different optical power levels from the microscope, shown in Table 2. The deposition rate exhibited a nearly synchronous increase of the movement speed of the nanosheets when the injected power (EDFA output power) was increased, shown in Fig. 5(b). Therefore we can reasonably reach the conclusion that the deposition rate

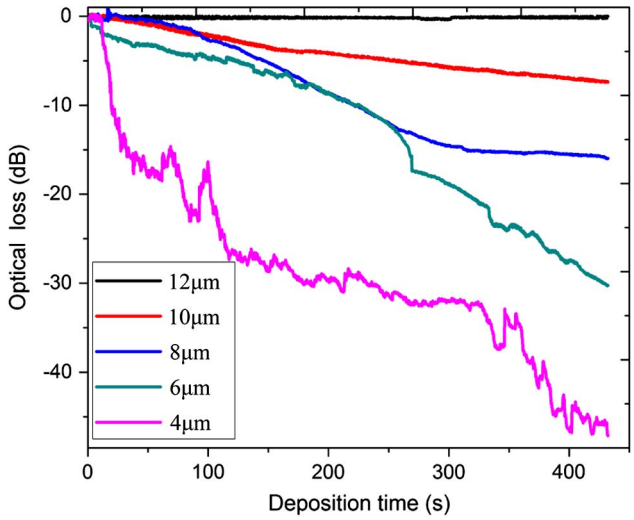

Fig. 6. Deposition process using different diameters of the tapered fiber.

was monotonically dependent on the movement speed of the nanosheets, which further demonstrated the influence of ethanol as a volatile solvent to increase the deposition rate.

4. DISCUSSION

To optimize the deposition process, it is important to investigate how different diameters of the tapered fiber affect the deposition results. Five different diameters of the tapered fiber, 4, 6, 8, 10, and 12 μm, were chosen for comparison. The optical power was fixed to 15 dBm, and MoS_2–ethanol dispersions were used. The measurement results are summarized in Fig. 6.

It can be observed that the deposition rate became faster with the decrease of the diameter. This was reasonable because more optical field was leaked outside the tapered fiber when the diameter was smaller. Thus MoS_2 nanosheets experienced stronger optical force during the deposition. When the diameter was larger than 12 μm, no deposition effect was observed. It is also interesting to observe that the evolution of the optical loss became more fluctuated with the decrease of the diameter. This was due to the fact that when the diameter was small, the scattering loss from the MoS_2 nanosheets became stronger and the deposited nanosheets were easier to remove when they collided with free-moving nanosheets. This fluctuation would make the deposition process difficult to control in the practical applications. The deposition rates for different diameters are summarized in Table 3. An optimized range of the diameters of the tapered fiber is 6–10 μm.

Furthermore, we have investigated the saturable absorption of MoS_2 deposited tapered fiber with a loss of 4.1 dB, shown in Fig. 7(a). It has a modulation depth of 2.3%, a

Table 2. Deposition Rates and Movement Speeds of the Nanosheets for Different Optical Power Levels

Optical power (dBm)	15	14	12	10	8	6	4	2	0
Deposition rate (dB/s)	0.087 ±0.021	0.063 ±0.020	0.057 ±0.016	0.038 ±0.009	0.017 ±0.005	0.009 ±0.002	0.004 ±0.002	0.001 ±0.001	0.000 ±0.001
Movement Speed (μm/s)	~8200	~6740	~3740	~1790	~1020	~480	~240	~100	~70

Table 3. Deposition Rates and Movement Speeds of the Nanosheets for Different Diameters

Diameter (μm)	4	6	8	10	12
Deposition rate (dB/s)	0.104 ± 0.065	0.056 ± 0.017	0.030 ± 0.011	0.016 ± 0.004	0.001 ± 0.0003
Movement speed (μm/s)	~9700	~4700	~2600	~980	~160

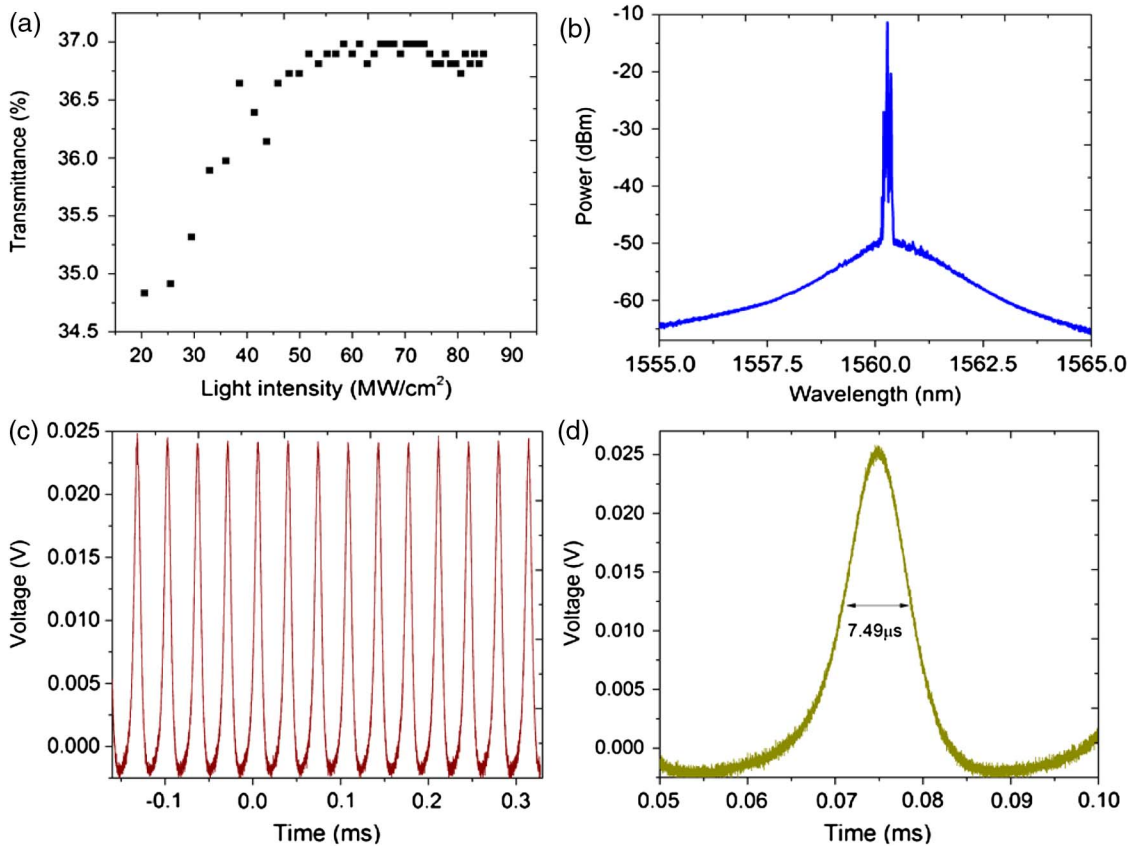

Fig. 7. (a) Saturable absorption of the MoS_2 deposited tapered fiber. (b) Optical spectrum of the *Q*-switched laser under 120 mW pump. (c) Pulse train of the *Q*-switched laser. (d) Single pulse profile.

saturable intensity of 60 MW/cm^2, and a nonsaturable loss of 63%. This result indicated the validity of the prepared MoS_2 deposited tapered fiber as a nonlinear device in photonic applications such as mode-locked lasers and *Q*-switched lasers. A demonstration of the MoS_2-based *Q*-switched laser was also provided. The laser output properties under 120 mW pump power are shown in Fig. 7(b) for optical spectrum and Figs. 7(c) and 7(d) for oscilloscope trace. The center frequency is 1560.2 nm, and the pulse duration is 7.49 μs.

5. CONCLUSIONS

In this paper, we have investigated the ECD of MoS_2 dispersions on the tapered fiber. The high volatility of the ethanol significantly increased the movement speed of the MoS_2 nanosheets and led to a deposition rate 2.6 times higher than that of DMF and a power threshold to drive the deposition as low as 4 dBm, whereas the deposition quality was nearly unaffected. Our findings demonstrated the effectiveness of the ECD method for a fast, easy, and controllable high-quality deposition. We believe our findings would also benefit the deposition of other similar materials on the tapered fiber, such as other types of TMDs.

ACKNOWLEDGMENTS

This work is partially supported by the Shanghai Yangfan Program (No. 14YF1401600), the State Key Lab Project of Shanghai Jiao Tong University (No. GKZD030033), the NSFC (Nos. 61178007 and 51302285), and the External Cooperation Program of BIC, CAS (No. 181231KYSB20130007). J. W. thanks the National 10000-Talent Program and the CAS 100-Talent Program for financial support.

REFERENCES

1. F. Bonaccorso, Z. Sun, T. Hasan, and A. C. Ferrari, "Graphene photonics and optoelectronics," Nat. Photonics **4**, 611–622 (2010).
2. Q. Bao, H. Zhang, Y. Wang, Z. Ni, Y. Yan, Z. X. Shen, K. P. Loh, and D. Y. Tang, "Atomic-layer graphene as a saturable absorber for ultrafast pulsed lasers," Adv. Funct. Mater. **19**, 3077–3083 (2009).
3. A. Martinez and Z. Sun, "Nanotube and graphene saturable absorbers for fibre lasers," Nat. Photonics **7**, 842–845 (2013).
4. J. N. Coleman, M. Lotya, A. O'Neill, S. D. Bergin, P. J. King, U. Khan, K. Young, A. Gaucher, S. De, R. J. Smith, I. V. Shvets, S. K. Arora, G. Stanton, H.-Y. Kim, K. Lee, G. T. Kim, G. S. Duesberg, T. Hallam, J. J. Boland, J. J. Wang, J. F. Donegan, J. C. Grunlan,

G. Moriarty, A. Shmeliov, R. J. Nicholls, J. M. Perkins, E. M. Grieveson, K. Theuwissen, D. W. McComb, P. D. Nellist, and V. Nicolosi, "Two-dimensional nanosheets produced by liquid exfoliation of layered materials," Science **331**, 568–571 (2011).
5. M. Liu, X. Yin, E. Ulin-Avila, B. Geng, T. Zentgraf, L. Ju, F. Wang, and X. Zhang, "A graphene-based broadband optical modulator," Nature **474**, 64–67 (2011).
6. Q. Bao, H. Zhang, B. Wang, Z. Ni, C. H. Y. X. Lim, Y. Wang, D. Y. Tang, and K. P. Loh, "Broadband graphene polarizer," Nat. Photonics **5**, 411–415 (2011).
7. H. Zhang, S. Lu, J. Zheng, J. Du, S. Wen, D. Tang, and K. Loh, "Molybdenum disulfide (MoS_2) as a broadband saturable absorber for ultra-fast photonics," Opt. Express **22**, 7249–7260 (2014).
8. H. Yu, H. Zhang, Y. Wang, C. Zhao, B. Wang, S. Wen, H. Zhang, and J. Wang, "Topological insulator as an optical modulator for pulsed solid-state lasers," Laser Photon. Rev. **7**, L77–L83 (2013).
9. K. Wang, J. Wang, J. Fan, M. Lotya, A. O'Neill, D. Fox, Y. Feng, X. Zhang, B. Jiang, Q. Zhao, H. Zhang, J. N. Coleman, L. Zhang, and W. J. Blau, "Ultrafast saturable absorption of two-dimensional MoS_2 nanosheets," ACS Nano **7**, 9260–9267 (2013).
10. J. Sotor, G. Sobon, K. Grodecki, and K. Abramski, "Mode-locked erbium-doped fiber laser based on evanescent field interaction with Sb_2Te_3 topological insulator," Appl. Phys. Lett. **104**, 251112 (2014).
11. Y.-W. Song, S.-Y. Jang, W.-S. Han, and M.-K. Bae, "Graphene mode-lockers for fiber lasers functioned with evanescent field interaction," Appl. Phys. Lett. **96**, 051122 (2010).
12. Z.-C. Luo, M. Liu, H. Liu, X.-W. Zheng, A.-P. Luo, C.-J. Zhao, H. Zhang, S.-C. Wen, and W.-C. Xu, "2 GHz passively harmonic mode-locked fiber laser by a microfiber-based topological insulator saturable absorber," Opt. Lett. **38**, 5212–5215 (2013).
13. Z. Luo, Y. Huang, J. Weng, H. Cheng, Z. Lin, B. Xu, Z. Cai, and H. Xu, "1.06 μm *Q*-switched ytterbium-doped fiber laser using few-layer topological insulator Bi_2Se_3 as a saturable absorber," Opt. Express **21**, 29516–29522 (2013).
14. M. Cizmeciyan, J. Kim, S. Bae, B. Hong, F. Rotermund, and A. Sennaroglu, "Graphene mode-locked femtosecond Cr:ZnSe laser at 2500 nm," Opt. Lett. **38**, 341–343 (2013).
15. R. Khazaeizhad, S. H. Kassani, H. Jeong, D.-I. Yeom, and K. Oh, "Mode-locking of Er-doped fiber laser using a multilayer MoS_2 thin film as a saturable absorber in both anomalous and normal dispersion regimes," Opt. Express **22**, 23732–23742 (2014).
16. R. I. Woodward, E. J. R. Kelleher, R. C. T. Howe, G. Hu, F. Torrisi, T. Hasan, S. V. Popov, and J. R. Taylor, "Tunable *Q*-switched fiber laser based on saturable edge-state absorption in few-layer molybdenum disulfide (MoS_2)," Opt. Express **22**, 31113–31122 (2014).
17. J. Liu, J. Xu, and P. Wang, "Graphene-based passively *Q*-switched 2 μm thulium-doped fiber laser," Opt. Commun. **285**, 5319–5322 (2012).
18. K. Wang, Y. Feng, C. Chang, J. Zhan, C. Wang, Q. Zhao, J. N. Coleman, L. Zhang, W. J. Blau, and J. Wang, "Broadband ultrafast nonlinear absorption and nonlinear refraction of layered molybdenum dichalcogenide semiconductors," Nanoscale **6**, 10530–10535 (2014).
19. H. Zhang, S. Virally, Q. Bao, L. K. Ping, S. Massar, N. Godbout, and P. Kockaert, "Z-scan measurement of the nonlinear refractive index of graphene," Opt. Lett. **37**, 1856–1858 (2012).
20. K. K. Chow, S. Yamashita, and S. Y. Set, "Four-wave-mixing-based wavelength conversion using a single-walled carbon-nanotube-deposited planar lightwave circuit waveguide," Opt. Lett. **35**, 2070–2072 (2010).
21. X. Zhang, S. Zhang, C. Chang, Y. Feng, Y. Li, N. Dong, K. Wang, L. Zhang, W. J. Blau, and J. Wang, "Facile fabrication of wafer-scale MoS_2 neat films with enhanced third-order nonlinear optical performance," Nanoscale **7**, 2978–2986 (2015).
22. Z. Luo, M. Zhou, J. Weng, G. Huang, H. Xu, C. Ye, and Z. Cai, "Graphene-based passively *Q*-switched dual-wavelength erbium-doped fiber laser," Opt. Lett. **35**, 3709–3711 (2010).
23. A. Martinez, K. Fuse, B. Xu, and S. Yamashita, "Optical deposition of graphene and carbon nanotubes in a fiber ferrule for passive mode-locked lasing," Opt. Express **18**, 23054–23061 (2010).
24. H. Liu, A.-P. Luo, F.-Z. Wang, R. Tang, M. Liu, Z.-C. Luo, W.-C. Xu, C.-J. Zhao, and H. Zhang, "Femtosecond pulse erbium-doped fiber laser by a few-layer MoS_2 saturable absorber," Opt. Lett. **39**, 4591–4594 (2014).
25. K. Kashiwagi and S. Yamashita, "Deposition of carbon nanotubes around microfiber via evanascent light," Opt. Express **17**, 18364–18370 (2009).